34th Annual International Conference of the IEEE EMBS
San Diego, California USA, 28 August - 1 September, 2012

A Head Motion Measurement System Suitable for 3D Cone-beam Tomography Using Markers

Ujjal Kumar Bhowmik and Reza R. Adhami, Senior *Member, IEEE*

***Abstract*—Head motion during brain CT studies can degrade the reconstructed image through distortion and other artifacts such as blurring, doubling and thereby contributing to misdiagnosis of diseases. Estimation of motion parameters is essential for mitigating motion artifacts. In this paper, we propose a marker based numerical optimization method to measure six degrees of freedom of head motion in three-dimensional cone-beam CT system without using any external motion sensors. Simulation results demonstrate that our method has prerequisite accuracy, linearity and range compared to the existing external sensor based method.**

I. Introduction

Patient head movement during brain CT remains a significant source of problems in three-dimensional brain imaging systems [1, 2]. It is essential that the head being scanned remains stable during data acquisition time. However, even with substantial amount of head restraint patient movement has frequently been reported in clinical applications. Therefore, it is essential to estimate parameters of motion (rotation and translation) during a CT scan so that they can be utilized to mitigate motion artifacts during the reconstruction process.

Over the past few years several methods have been proposed to detect motion in brain CT. Goldstein et al. [3] proposed a method that uses a triad of three incandescent lights attached to the patient's head while viewed by two position sensitive optical sensors. Fulton et al. [4] also proposed a similar approach that uses infrared reflector and detector. On the other hand, several other approaches solely based on Sinogram/Linogram information [5, 6] have been reported in the literature. It must be noted that motion detection using external sensors could cause systematic biases in the reconstructed images and Sinogram approaches often fails to detect motion in the case of substantial head motion. Therefore, we propose a marker based motion detector system to detect and quantify head motion. Simulation results validate the accuracy and linearity of our system.

This paper is organized as follows. In section II, we give a brief description of our Marker Based Motion Detector system (MBMD). In section III, we illustrate the MBMD system. In section IV, we discuss briefly the iteration technique we used for our numerical optimization. Finally in section V, we validate our MBMD system with computer simulation results.

U. Bhowmik and R. Adhami are with the Department of Electrical and Computer Engineering, The University of Alabama in Huntsville, AL 35899 USA. (email: ukb0001@uah.edu, rradhami@eng.uah.edu).

II. Marker Based Motion Detector (MBMD)

The idea behind our motion detection system is to detect head motion during CT scan without using any external optical motion tracking sensors. The proposed system, which is implemented in circular cone-beam CT assembly, as shown in Fig. 1, uses four markers to detect rotational and translational parameters (six degrees of freedom) of motion. In Circular cone-beam CT system the source-detector pair rotates in a circular orbit about Z-axis with a suitable step size, w.r.t. Y-axis and at every source-detector position the source emits a cone-beam of rays which passes through the object and creates an X-ray projection on the detector plate. In our proposed system, four markers are to be attached on a head surface using a suitable head band in such a way that their positions (3D coordinates) will always be linearly independent and their projections on the X-ray detector plate will never cross each other in case of any practical head motion. Number of markers and their linear independence are

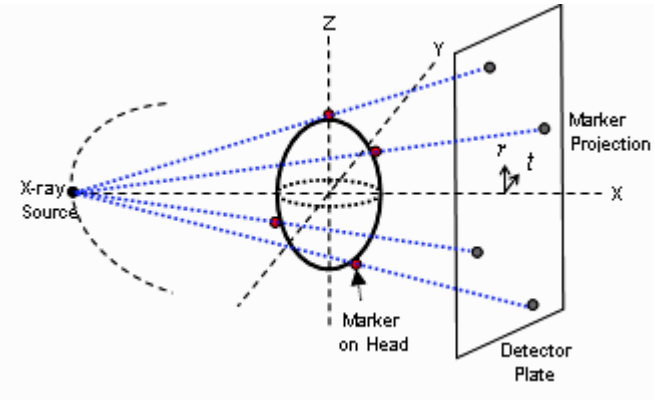

Figure 1. Cone-beam CT assembly with markers

the two necessary conditions for finding the motion parameters. Coordinates of markers on head and their corresponding projections on detector plate are known for motion free ideal case. In case of any head motion during CT scan, the markers and their corresponding projections will shift from their ideal positions. However, the relative distances between the markers will always remain constant because of the rigid body structure. The new positions of the projections of markers are known from the detector plate but the new positions of the markers are not known. In this proposed MBMD system, the new positions of the shifted markers are estimated by a numerical iterative optimization technique which minimizes the differences between the known relative distances among the marker positions and the corresponding relative distances among the estimated markers positions. Once the new positions of the shifted markers are known, the motion parameters can easily be

calculated from the estimated shifted marker positions and their corresponding ideal marker positions.

III. Illustration of the MBMD System

In order to make our calculation easier, the Source, Detector and the Markers coordinates are represented in the same coordinate system, as shown in Fig. 2, where the Source is considered as the origin of the coordinate system. Our proposed MBMD system is illustrated step by step in the following section:

1) We have four points, $(x_i y_i z_i,\ where\ i = 1,2,3,4)$, which we call markers (Figs. 2 & 3.), in three dimensional coordinate system. We know their coordinates.
2) From one point in space (0,0,0), which we call X-ray source, we draw four lines (1.1) through the four markers. These lines will intersect a plane, which we call X-ray detector. We know the coordinates of four intersection points, $(\bar{x}_i\ \bar{y}_i \bar{z}_i,\ where\ i = 1,2,3,4)$, which we call marker projections on the detector plate (Fig. 4).

$$\frac{x}{y} = \frac{\bar{x}_i}{\bar{y}_i}, \qquad \frac{y}{z} = \frac{\bar{y}_i}{\bar{z}_i} \tag{1.1}$$

3) Now the four points (Markers) are shifted because of motion. We don't know the coordinate of the shifted markers, $\left(x'_i y'_i z'_i\right)$, anymore. The only thing we know is that the relative distances (1.2 and 1.3), as shown in Fig. 3, between the markers are fixed because of solid body.

$$\sqrt{(x_i - x_j)^2 + (y_i - y_j)^2 + (z_i - z_j)^2} = d_{ij} \tag{1.2}$$

$$\sqrt{(x'_i - x'_j)^2 + (y'_i - y'_j)^2 + (z'_i - z'_j)^2} = d_{ij} \tag{1.3}$$

$$for\ \forall\ j > i$$

Where,

$$i = 1,2,3\ and\ j = 2,3,4$$

4) Now if we draw four lines (1.4) from the Source through these four shifted markers they will intersect the same plate, X-ray detector, in four new points, $(\bar{x}_i'\ \bar{y}_i' \bar{z}_i'\ where\ i = 1,2,3,4)$. We know the coordinate of these four intersection points (Fig. 4).

$$\frac{x}{y} = \frac{\bar{x}'_i}{\bar{y}'_i}, \qquad \frac{y}{z} = \frac{\bar{y}'_i}{\bar{z}'_i} \tag{1.4}$$

5) Our goal is to find the coordinates of the shifted markers, $\left(x'_i y'_i z'_i\ \ where\ i = 1,2,3,4\right)$, from the information described in 1, 2, 3, and 4.

In other words, our problem boils down to calculating (4×3) =12 coordinates of the four shifted markers from six relative distances (Euclidean distances) between the markers and four straight line (linear in x, y and z) equations. This system of equation is solved numerically by the following iterative optimization technique.

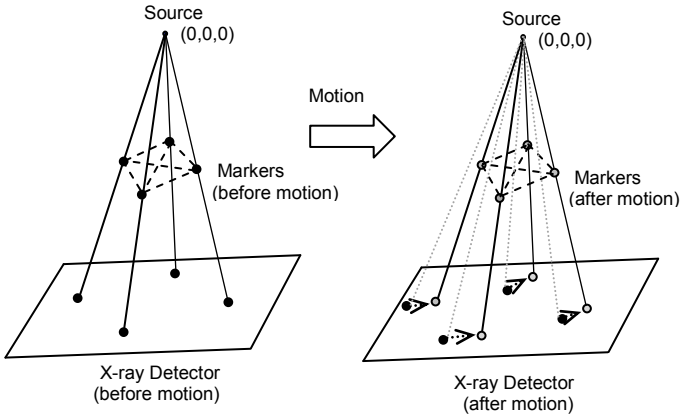

Figure 2. Source, Detector and Markers showing motion

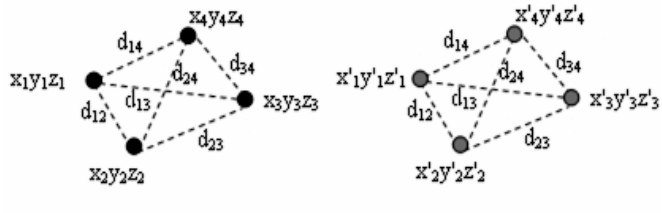

Figure 3. Relative Distances between Markers (Left-before motion, Right-after motion)

IV. Numerical Iterative Optimization

The first step in our numerical optimization technique is to find the shifted markers approximate positions, $(x_i''\ y_i''\ z_i'',\ \ where\ i = 1,2,3,4)$. As shown in Fig. 4, the approximate position of the shifted marker1 can be found by drawing a line, which is parallel to the line between the projections $(\bar{x}_1\ \bar{y}_1 \bar{z}_1)$ and $(\bar{x}_1'\ \bar{y}_1' \bar{z}_1')$, from its ideal marker position to the shifted line. The intersection point, $\left(x_1''\ y_1''\ z_1''\right)$, is the approximate position of the shifted marker1. The generalized formula for finding the approximate positions of the shifted markers is given by (1.5)

$$z_i'' = \frac{K_{i2} \pm \sqrt{K_{i2}^2 - 4K_{i1}K_{i3}}}{2K_{i3}} \quad \begin{cases} + if\ z_i\ is\ positive \\ - if\ z_i\ is\ negative \end{cases}$$

$$y_i'' = z_i'' \frac{\bar{x}'_i}{\bar{z}'_i} \qquad ; \qquad x_i'' = z_i'' \frac{\bar{y}'_i}{\bar{z}'_i} \tag{1.5}$$

Where,

$$i = 1,2,3,4$$

$$K_{i1} = (x_i^2 + y_i^2 + z_i^2) - d_{isp}^2$$

$$K_{i2} = \left(2x_i \frac{\bar{x}'_i}{\bar{z}'_i} + 2y_i \frac{\bar{y}'_i}{\bar{z}'_i} + 2z_i\right)$$

$$K_{i3} = \left(\frac{\bar{x}_i'^2}{\bar{z}_i'^2} + \frac{\bar{y}_i'^2}{\bar{z}_i'^2} + 1\right)$$

$$d_{isp} = \frac{d_{is}}{K} \quad ; \ K = \frac{SDD}{x_i}$$

$$d_{is} = \sqrt{(\bar{x}_i - \bar{x}'_i)^2 + (\bar{y}_i - \bar{y}'_i)^2 + (\bar{z}_i - \bar{z}'_i)^2}$$

SDD is the distance between the source and the detector

After finding the approximate marker positions, ($x_i''\ y_i''\ z_i''$), we need to calculate the relative distances, d_{ij}'', between them (1.6).

$$d_{ij}'' = \sqrt{\left(x_i'' - x_j''\right)^2 + \left(y_i'' - y_j''\right)^2 + \left(z_i'' - z_j''\right)^2} \quad (1.6)$$
$$for\ \forall\ j > i$$

Where,

$$i = 1,2,3\ and\ j = 2,3,4$$

If these relatives distances, d_{ij}'' , are close to the d_{ij} (relative distances between the ideal marker positions), then our approximation is good. Otherwise, we need to vary the positions of the approximate markers positions along their corresponding shifted lines so that their relative distances become very close to the ideal distances, d_{ij}. Once we reach within our error limit, in other words, when

$\sum_{ij} abs\left(d_{ij}'' - d_{ij}\right) \leq Error$, we can claim,

$$x_i'' = x_i',\ y_i'' = y_i',\ z_i'' = z_i' \quad where\ i = 1,2,3,4 \quad (1.7)$$

After finding the shifted marker positions, $\left(x'_i y'_i z'_i\right)$, we can easily extract the motion parameters from the following equation (1.8):

$$\begin{bmatrix} x_1 & x_2 & x_3 & x_4 \\ y_1 & y_2 & y_3 & y_4 \\ z_1 & z_2 & z_3 & z_4 \\ 1 & 1 & 1 & 1 \end{bmatrix} = \begin{bmatrix} r_{11} & r_{12} & r_{13} & t_{xe} \\ r_{21} & r_{22} & r_{23} & t_{ye} \\ r_{31} & r_{32} & r_{33} & t_{ze} \\ 0 & 0 & 0 & 1 \end{bmatrix} \times \begin{bmatrix} x_1' & x_2' & x_3' & x_4' \\ y_1' & y_2' & y_3' & y_4' \\ z_1' & z_2' & z_3' & z_4' \\ 1 & 1 & 1 & 1 \end{bmatrix} \quad (1.8)$$

Where,

$$r_{11} = \cos\alpha_e \cos\vartheta_e \qquad r_{21} = \sin\alpha_e \cos\vartheta_e$$
$$r_{32} = \sin\delta_e \cos\vartheta_e \qquad r_{33} = \cos\vartheta_e \cos\delta_e$$
$$r_{12} = \cos\alpha_e \sin\vartheta_e \sin\delta_e - \cos\delta_e \sin\alpha_e$$
$$r_{13} = \cos\alpha_e \sin\vartheta_e \cos\delta_e - \sin\alpha_e \sin\delta_e$$
$$r_{22} = \sin\alpha_e \sin\vartheta_e \sin\delta_e + \cos\alpha_e \cos\delta_e$$
$$r_{23} = \sin\alpha_e \sin\vartheta_e \cos\delta_e - \cos\alpha_e \sin\delta_e$$
$$r_{31} = -\sin\vartheta_e$$

The six degrees of freedom of motion are:

$$\alpha_e - rotation\ about\ z\ (yaw)$$
$$\vartheta_e - rotation\ about\ y\ (pitch)$$
$$\delta_e - rotation\ about\ x\ (roll) \qquad and$$
$$t_{xe}, t_{ye}, t_{ze}\ are\ the\ translation\ parameters$$

Since the marker coordinates are linearly independent for any form of practical motion, solution of (1.8) will always exist.

Iteration Steps: We choose some approximated line segment (L) of the shifted line around ($x_i''\ y_i''\ z_i''$) as the location where a marker can take possible position after motion. Though we can choose maximum possible length of the shifted line for our iteration but in order to get faster convergence we choose this smaller length L. L could be chosen based on the initial knowledge of the amount of head movement which can be guessed either from the distance between ideal and shifted marker projections or from the -

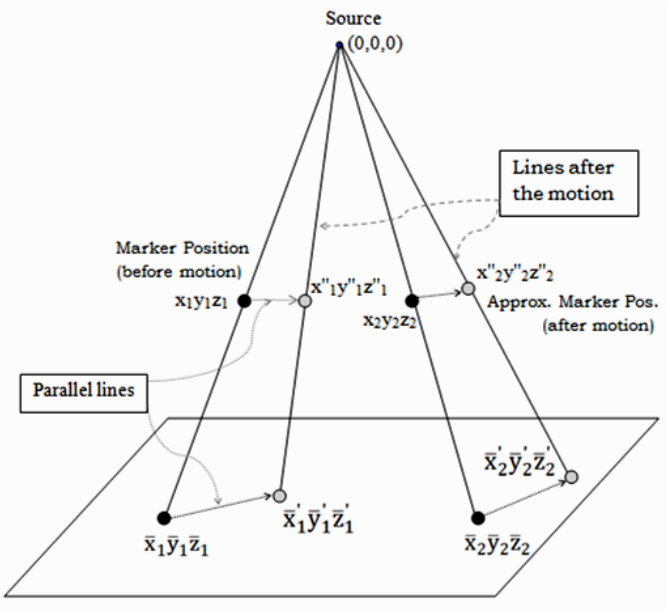

Figure 4. Approximate coordinates of two markers after motion

correlations between the adjacent X-ray projections of head [2]. After choosing L, we divide the length into N equal parts for our iteration. Obviously, large values of N will produce better accuracy. Considering each N point as the possible position of a marker, iteration is performed in several stages. In the first stage, using L, we try to find the closest possible coarse solution (i.e approximate coordinates of the shifted marker position). After getting the closest possible coarse marker position, we choose a smaller length, half of previous length (L/2), around the estimated coarse marker position and divide it again by N equal parts for the next iteration (we used N=100). The process is repeated until we reach the desired *Error* margin. If the process doesn't converge, we need to increase L and the number of iteration.

V. Simulation Results

The necessary geometric parameters and the initial marker positions (which are placed on the surface of a 3D object) w.r.t. the origin of the 3D object, as listed in Table 1, are used for our simulation.

Table 1. Geometric parameters of Cone-beam system

Geometric Parameters		Initial Marker Positions		
SDD (Source to detector distance)	2000 cm	x(cm)	y(cm)	z(cm)
SAD (Source to phantom distance)	1600 cm	0	0	9.25
Detector size 25.6× 25.6cm^2		7.25	0	3.25
Reconstruction Grid Volume 20.48×20.48×20.48 cm^3		0	-7.25	-3.25
		-4.75	4.75	-9.25

The performance of our proposed MBMD system is tested in two stages. In the 1st stage, the performance of the MBMD is tested with a known set of combined motion. We perturb the 3D object with translational (t_x = 1cm, t_y = 2cm, t_z = 1.5cm) and rotational motion (*roll* = 15°, *pitch* = 20°, *yaw* = 25°) at different source-detector positions (β) during data acquisition time. Simulation results of actual and estimated motion parameters are listed in table 2. Estimated translation

motion parameters are within 1.5% of the actual values and estimated rotational parameters are within 0.1% of the actual values. We use *Error Limit* = 0.002 for our iteration.

Table 2. Comaprisons of estimated and actual motion parameters

	Motion Parameters	$\beta = 160$	$\beta = 180$	$\beta = 200$
Estimated	t_{xe} (cm)	1.0036	0.9945	1.0037
	t_{ye} (cm)	1.7047e-009	2.0000	2.0000
	t_{ze} (cm)	-5.1528e-009	9.5482e-008	1.5000
	Pitch (ϑ_e^{o})	2.2245e-007	20.0009	20.0010
	Roll (δ_e^{o})	15.0000	14.9999	15.0000
	Yaw (α_e^{o})	5.7943e-008	-2.9808e-007	24.9991
Actual	t_x (cm)	1.0	1.0	1.0
	t_y (cm)	0.0	2.0	2.0
	t_z (cm)	0.0	0.0	1.5
	Pitch (ϑ^{o})	0.0	20.00	20.00
	Roll (δ^{o})	15.00	15.00	15.00
	Yaw (α^{o})	0.0	0.0	25.00

In 2nd stage, the linearity and accuracy of our MBMD system is tested with six known sets of gradual variation of motions (3 rotational and 3 translational). For rotational motion corruption case, the 3D object is perturbed with a range of roll, pitch, and yaw motion parameters (-5° to 5°) individually in three separate test scans. For translational case, the object is perturbed with a range of axial, lateral, and vertical motion parameters (-6mm to +6mm) individually in three separate test scans. The results of our simulation are plotted (zoomed in) in Fig. 5. A comparison of the results with the published results of well known Goldstein *et al.* [3] optical sensor method is also given in table 3. Where, we have compared the slopes and the square correlation coefficient (R^2) of the best fit lines through the data points. The results demonstrate that the system is linear, with most slopes being within 1% of unity. The rms deviations of the MBMD data from the best-fit straight lines are less then 0.01° for all rotation angles (±5°) and less than 0.02mm for the translations (±6mm). The rms deviation from the actual input is less than 0.02° and 0.03cm for rotation and translation, respectively. The simulation results of square correlation coefficients (R^2) of the best fit lines through the data points demonstrate that the MBMD estimated data represent the real data values much better than the Goldstein method.

VI. Conclusion

In this paper, we have designed and implemented an innovative marker based motion detection system which gives better performance in comparison with the well-known optical sensor based method. Simulation results demonstrate that our MBMD has requisite accuracy, linearity, resolution and range. Our proposed method could also tackle abrupt and large variation of motion. We have verified our system on synthetic data set only. In our future endeavor, efforts will be made to implement the MBMD on a real life data set and to establish the clinical significance of this technique.

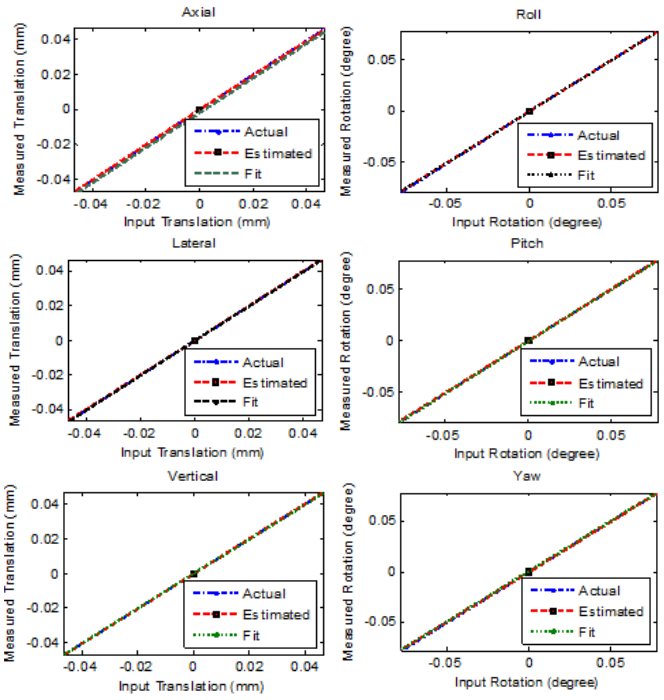

Figure 5. Linearity and Accuracy of MBMD system

Table 3. Comparison of results showing linearity and accuracy

Motion	Slope		R^2	
	Goldstein	MBMD	Goldstein	MBMD
Axial	0.983±0.004	0.9999±0.00337	0.99987	0.9998
Lateral	0.993±0.003	1.0000±0.00019	0.99998	1.0000
Vertical	1.004±0.002	1.0000±0.00030	0.99987	1.0000
Roll	0.990±0.002	0.9999±0.00001	0.99996	0.9999
Pitch	0.904±0.011	1.0000±0.00005	0.99904	1.0000
Yaw	0.991±0.009	1.0000±0.00010	0.99944	0.9999

References

[1] U. Bhowmik and R. Adhami, "A Correlation and LS-SVM Based Approach to Mitigate Motion Artifacts in FDK Based 3D Cone-Beam Tomography," *International Conference of the IEEE Engineering in Medicine and Biology Society (EMBC '11)*, Boston, USA.

[2] U. Bhowmik, and R. Adhami, "Motion Artifacts Compensation in FDK based 3D cone-beam Tomography Using Correlation of X-Ray Projections," *Proceedings of The International Conference on Image Processing, Computer Vision & Pattern Recognition (IPCV 2011),* Vol. 1, pp 407-413, Las Vegas, USA.

[3] R. Goldstein, E. Margaret, and W. Dube, "A Head Motion Measurement System Suitable for Emission Computed Tomography," *IEEE Trans. Of Medical Imaging,* Vol. 16, No. 1, pp 17-27, February 1997.

[4] R.R. Fulton, S. Eberl, S.R. Meikle, M. Braun, "A Practical 3D Tomographic Method for Correcting Patient Head Motion in Clinical SPECT," *IEEE Trans. On Nuclear Science*, Vol. 46, No. 3, June 1999.

[5] S. Sarkar, M. A. Oghabian, I. Mohammadi, A. Mohammadpour, and A. Rahmim , "A Linogram/Sinogram Cross-Correlation Method for Motion Correction in Planar and SPECT Imaging," *IEEE Trans. On Nuclear Science,* Vol. 54, No. 1, February 2007.

[6] L. Weiguo and R. Mackie, "Tomographic Motion Detection and Correction Directly in Sinogram space," *Phys. Med. Biol*, Vol. 47, pp- 1267-1284, 2002.